



Total Control

*Advanced integrated supervisory and wind turbine control
for optimal operation of large Wind Power Plants*

Coupling of Gaussian wake merging to
background ABL model

D1.8

Delivery date: 24.08.2020
Lead beneficiary: KUL
Dissemination level: Public



This project has received funding
from the European Union's Horizon
2020 Research and Innovation
Programme under grant agreement
No. 727680

Author(s) information (alphabetical):		
Name	Organisation	Email
Johan Meyers	KUL	johan.meyers@kuleuven.be
Ishaan Sood	KUL	ishaan.sood@kuleuven.be
Lucca Lanzilao	KUL	

Document information

Version	Date	Description	Reviewed by	Approved by
1	24.08.2020	Prepared by Ishaan Sood	Reviewed by Johan Meyers Gunner Chr. Larsen	Approved by Johan Meyers

TABLE OF CONTENTS

1.	Introduction	4
2.	Model Methodology	4
3.	Simulation cases.....	4
4.	Results.....	7
5.	Conclusions	9
	REFERENCES	9

1. INTRODUCTION

One of the core activities within the TotalControl project is the development and validation of appropriate end-to-end wind-farm simulation models to develop and test new wind farm control strategies. While high-fidelity Large Eddy Simulation (LES) tools provide a means for taking numerical measurements under controlled conditions, the large computational cost associated with these simulations can be prohibitive for control and design purposes. To this end, a fast boundary layer model, from here on called the Three Layer Model (TLM), has been developed and coupled with a Gaussian windfarm force model to enable faster study of wind farm response in different atmospheric conditions.

The current report discusses the validation of the TLM against LES datasets previously generated during the TotalControl project. Subsets of the TotalControl LES flow database, which contains unsteady three-dimensional flow data of unperturbed atmospheric boundary layers (i.e. without the influence of turbines) are utilized to simulate the atmospheric conditions in the TLM and fed into the TotalControl reference wind farm. The resulting power output is compared against the LES windfarm database for validation of the model.

The report is structured as follows. Section 2 details the methodology of the TLM and the coupling of the windfarm force model with the background atmospheric model. Section 3 outlines the selected simulation cases for validation and the included setup. Finally, the results and validation are presented in the last section.

2. MODEL METHODOLOGY

The TLM divides the vertical structure of the atmosphere into three layers – thus, the name three-layer model (TLM). The atmospheric boundary layer (ABL) is divided into two regions: the wind-farm layer, which simulates the lowest region of the atmosphere, where the wind turbine forces are felt directly, and an upper layer which is only indirectly affected by the wind farm through vertical turbulent transport of momentum. The third layer accounts for the free atmosphere aloft the ABL. For further details about the TLM see Allaerts and Meyers (2019).

The Gaussian wake model (GWM) (Niayifar and Porté-Agel, 2016), which is an analytical wake merging model, is used to account for turbine wake interactions. The inputs of this model are the turbine location, turbine rotor diameter, turbine hub height and the thrust curve. The turbine data of the DTU 10MW turbine are utilized (Bak et al 2013). A two-way coupling between the TLM and the wake model is established (see Allaerts and Meyers (2019)), connecting local turbine inflow velocities to global height average TLM velocities. The resulting model (GWM+TLM) accounts for turbine–turbine interactions, wind-farm wakes and gravity-wave effects. We further improved the model for computational efficiency, such that the time taken for one wind-farm simulation with the TLM is comparable to evaluation times of classical engineering wake models, such as the Jensen model.

The TLM equations are discretized using a Fourier-Galerkin spectral technique, hence periodic boundary conditions at the edges of the computational domain are used. The computational domain has a dimension of 500 x 500 km² so that perturbations die out before being recycled, and a grid resolution of 200 m is adopted. The TLM solution has been proofed to be grid-independent (Allaerts and Meyers, 2019), hence no benefit would be provided by finer grids.

Results of the TLM have been previously successfully validated against those of SP-Wind, a wind-farm Large Eddy Simulation (LES) code built on a high-order flow solver developed over the last 10 years at KU Leuven (Calaf, Meneveau & Meyers 2010; Munters, Meneveau & Meyers 2016; Allaerts & Meyers 2017, Allaerts & Meyers 2019). In this report, specific cases previously simulated using SP-Wind in the context of the TotalControl project are now simulated in the TLM for further validation. In particular, in earlier work, LES reference cases were constructed using spanwise periodic boundary conditions, leading to wind farms with a spanwise infinite extend. The new simulations used here, consist of fully finite wind farms.

3. SIMULATION CASES

The TotalControl Reference Wind Power Plant (TC RWP) has been defined in deliverable D1_03 (Andersen et al., 2018). The TC RWP consists of 32 turbines in a staggered pattern, see *Figure 1*. The choice of a staggered pattern is somewhat arbitrary; but it makes sense to arrange the turbines in this manner if the prevailing wind direction were from the left.

The reference turbines are the DTU 10 MW turbines (Bak et al., 2013), with a hub height of 119 m and a rotor diameter of 178.3 m.

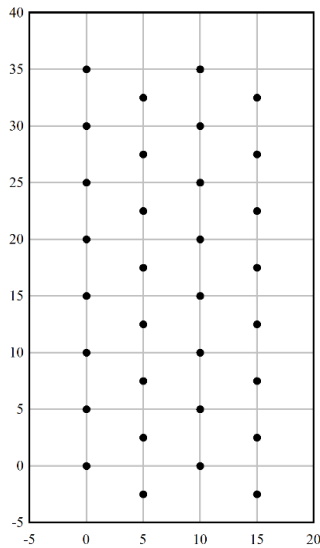


Figure 1: Layout of the TC RWP. Axes have units of s/D , with a rotor diameter $D = 178.3$ m.

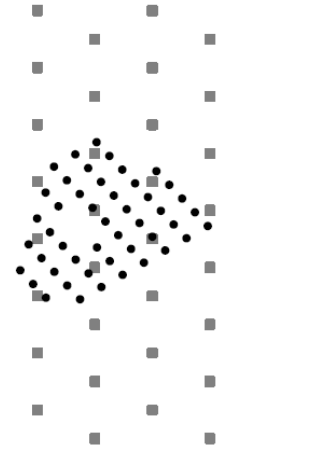


Figure 2: Scale comparison of the TC RWP (gray) and the Lillgrund WP (black)

The number of turbines results from a compromise between limiting the computational cost of high-resolution flow simulations and having an array that is large enough to be relevant as an offshore wind power plant. Figure 2 shows a scale comparison of the TC RWP to the Lillgrund plant, also featured in the TotalControl project.

The columns of eight turbines (vertical in Figure 1) provide a "long" direction where the turbine-to-turbine wake effects can approach their asymptotic values. Furthermore, given a top-down wind direction a typical aligned layout is achieved, for which wake redirection was found to be a very efficient wind-farm control strategy (Munters and Meyers 2018). In the perpendicular "short" direction (horizontal in Figure 1) only two turbines are directly aligned. For a left-right wind direction, a standard staggered configuration is achieved, for which wake induction control strategies have been found to be more suitable. In this way, both the redirection and induction approach to wind-farm control can be investigated without a priori favouring one over the other based on wind-farm layout. Different wind inflow directions can be achieved by rotating the entire wind farm by the desired inflow angle, e.g. 30 and 60 degree cases (Figure 3).

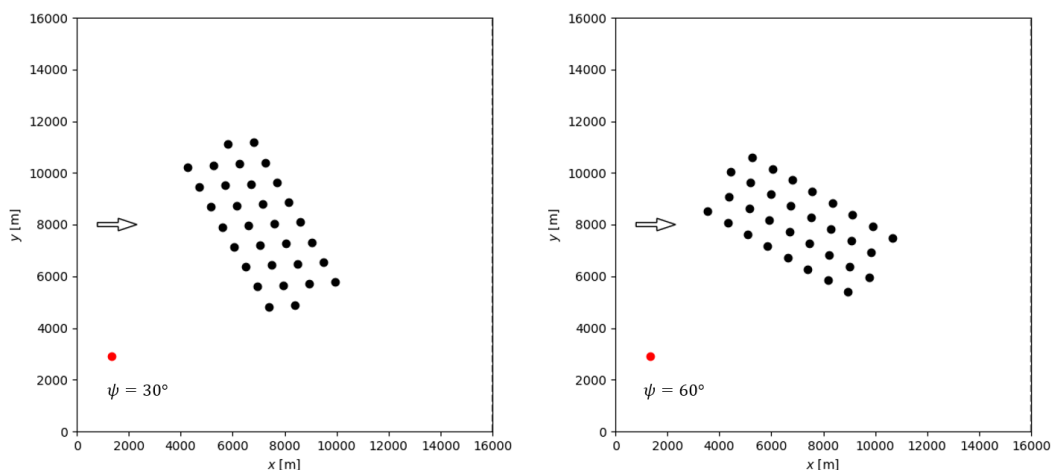


Figure 3 Reference wind farm rotated by a) 30 and b) 60 degrees to simulate different inflow wind directions

The precursor data included in the TotalControl flow database has been used to specify the atmospheric conditions in the TLM to facilitate a direct comparison between the results from the TLM and SP-Wind. The precursor data contains unsteady three-dimensional flow data of an unperturbed atmospheric boundary layer (i.e. without the influence of turbines). This data is interpolated and fit into the TLM to determine the inflow velocities in the different layers of the model. The precursor data of atmospheric boundary layer simulations is publicly available in the online zenodo repository at <https://zenodo.org/communities/totalcontrolflowdatabase/>. The windfarm output data which has been simulated using the precursor data is available at <https://zenodo.org/communities/totalcontrolwindfarmdatabase/>.

Detailed description of the precursor simulations have already been presented in the D 1.04 part 1 report, available at : <https://cordis.europa.eu/project/id/727680/results>. Of the described precursor cases, the conventionally neutral boundary layer (CNBL) cases are utilized in this report for validation of results. CNBL is a neutral boundary layer, capped by a strongly stable inversion layer. Above the CNBL, the free atmosphere is stably stratified with a constant potential temperature gradient.

The initial conditions for the mean wind velocity vector along the domain height as well as the temperature are shown for the CNk2 and CNk4 cases in figure 4. The figure shows the smooth transition between the velocities and temperatures in the boundary layer (characterized by veered and sheared velocities with well-mixed temperature) and in the free atmosphere above the capping inversion (with uniform velocities and stable free-atmosphere stratification).

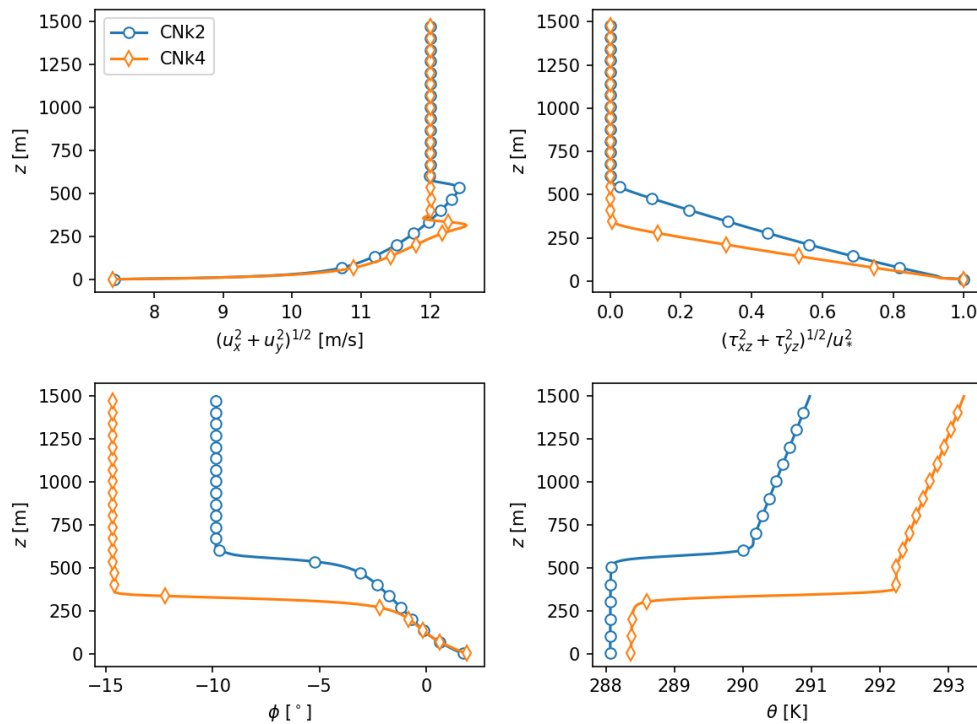


Figure 4: Flow profiles for KU Leuven CNBL cases with varying boundary layer heights. Top left: Horizontal velocity. Top right: Total (resolved + subgrid) shear stress. Bottom left: Wind veer. Bottom right: Potential temperature.

Utilizing different combinations of the available CNBL flow data and windfarm rotation angle, windfarm performance under different atmospheric conditions and wind directions can be studied. Table 1 specifies the parameters of the different cases simulated in the TLM.

Table 1: CNBL cases

Inflows			
CNk2	$z_0 = 2 \times 10^{-4} \text{ m}$	$\Delta\theta = 2\text{K} (h = 500 \text{ m})$	
CNk4	$z_0 = 2 \times 10^{-4} \text{ m}$	$\Delta\theta = 4\text{K} (h = 250 \text{ m})$	
Simulation cases			
CNk2 30	$\psi = 30^\circ$	$V_\infty = 11 \text{ m/s} (h = 119\text{m})$	
CNk2 60	$\psi = 60^\circ$	$V_\infty = 11 \text{ m/s} (h = 119\text{m})$	
CNk4 30	$\psi = 30^\circ$	$V_\infty = 11.3 \text{ m/s} (h = 119\text{m})$	
CNk4 90	$\psi = 90^\circ$	$V_\infty = 11.3 \text{ m/s} (h = 119\text{m})$	

4. RESULTS

The velocity deficit in the domain in the 4 simulated cases are presented in Figure 5. As expected, strong wake deficits exist behind the windfarm, with the 60 and 90 degree orientation cases exhibiting larger wake deficit due to a greater number of aligned turbines as compared to the 30 degree orientation. Velocity deficits in LES simulations using SP-Wind for the same cases are presented in Figure 6. The LES domain size is 16 km by 16 km, and a grid resolution is 13 m is adopted. A fringe region, where turbulent inflow conditions are introduced to the domain, is applied in the last 10% of the domain to overcome periodic boundary conditions. Good comparison can be seen in the velocity deficits observed by TLM and SP-Wind for all the simulated cases.

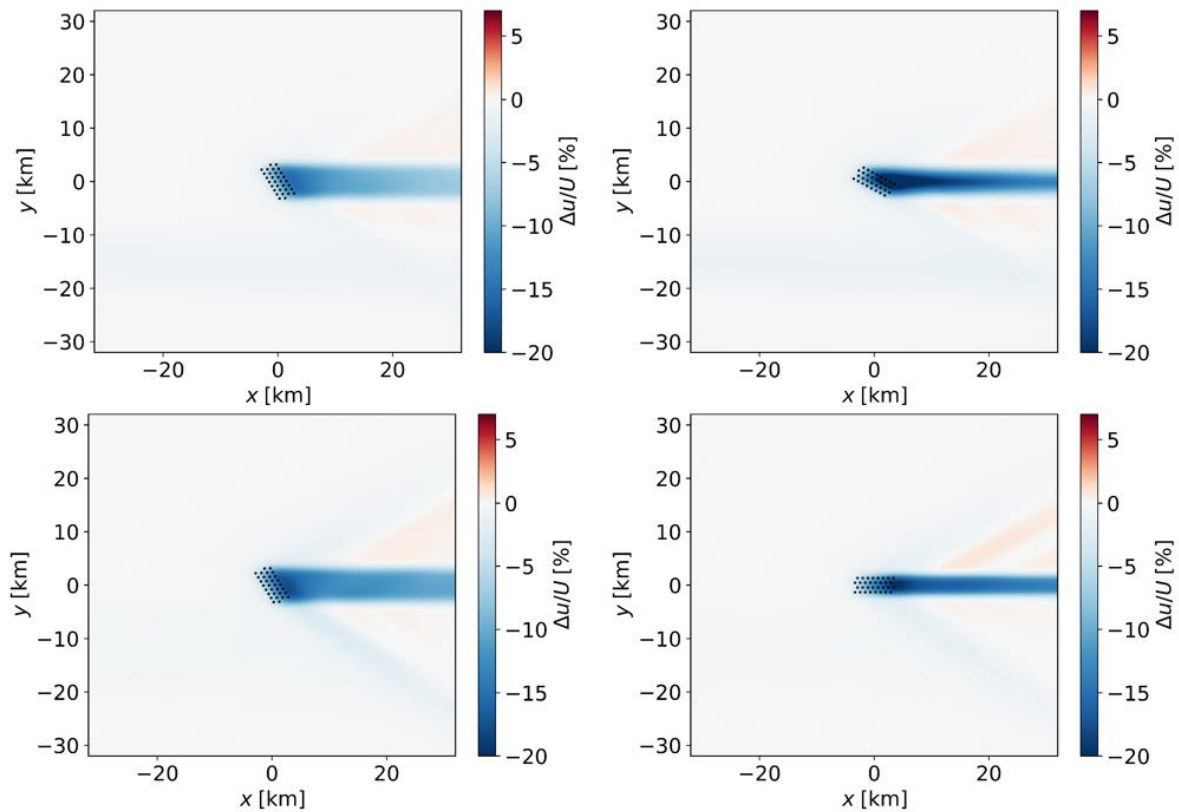


Figure 5 Velocity deficit results from TLM. Top left : CNk2 30 Top right: CNk2 60 Bottom left: CNk4 30 Bottom right : CNk4 90

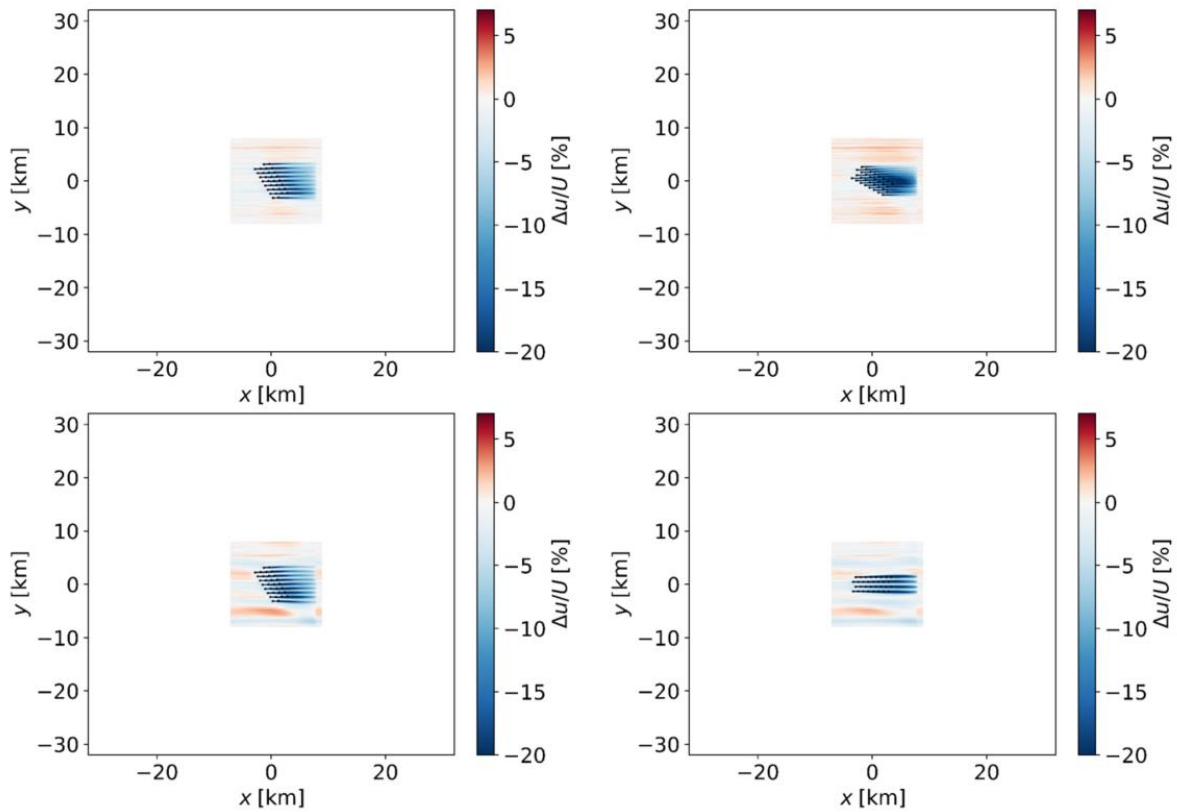


Figure 6 Velocity deficit results from LES. Top left : CNk2 30 Top right: CNk2 60 Bottom left: CNk4 30 Bottom right : CNk4 90

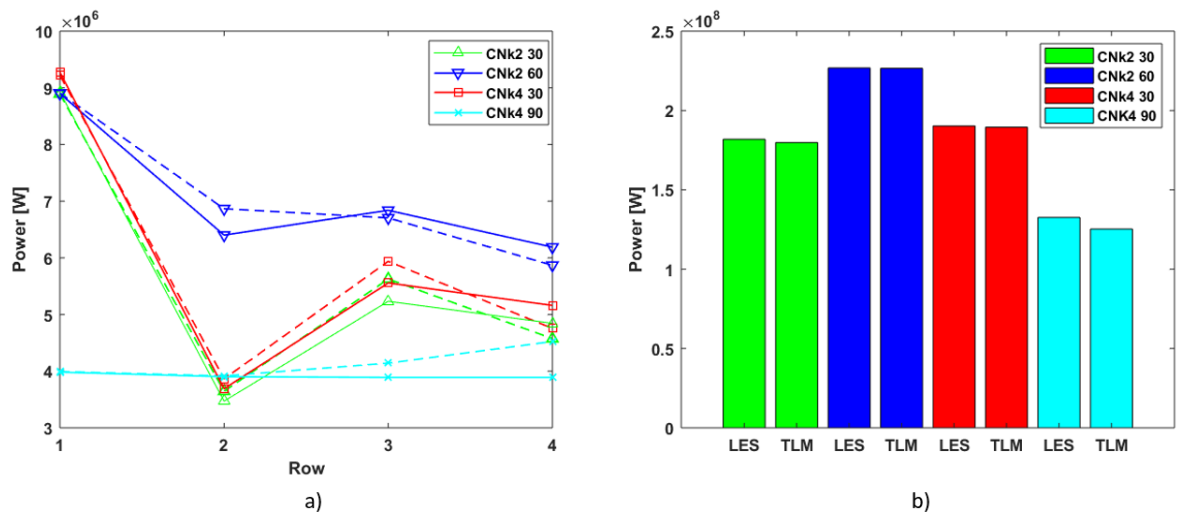


Figure 7 Comparison of power output results between TLM and SP-Wind. a) Row power comparison ,LES results are represented by dashed lines and TLM results are solid lines. b) Total windfarm power output comparison

A comparison between the wind farm power output from TLM are presented against results from LES simulations of SP-Wind in Figure 6. Wind turbines in SP-Wind are modeled using an aeroelastic actuator sector model, coupled with a nonlinear flexible multi-body dynamics model (Vitsas and Meyers 2016). The LES simulations with windfarms were run for 3600 seconds during which turbine performance data was collected. Excellent comparison can be seen in the total windfarm power output between the two codes in Figure 6 b) for all the considered cases. A row-wise power production comparison is shown in Figure 6 a), where the rows are numbered in increasing order from left to right in the orientation showed in Figure 1. It can be seen that TLM exhibits the same trends in power production across the

rows when compared to the LES results. The CNk2 60 case has highest average row power in downstream rows, due to the largest number of turbines operating in un-waked conditions in this configuration. Conversely, the 90° cases have the lowest row average power due to a fully aligned configuration. While the first row power compares almost exactly for the two codes, slight variations can be seen in power output in the downstream rows between the TLM and SP-Wind results, being most significant in the fully aligned CNk4 90 case. This could be attributed to an averaging error in the LES time series output and also due to an imperfect fit of the analytical wake turbulent intensity expression adopted directly from Niayifar, A. and Porté-Agel.

5. CONCLUSIONS

A validation study was performed between the fast TLM code and SP-Wind, comparing windfarm simulation results in the context of the TotalControl project. The TLM code utilizes a Gaussian Wake Merging (GWM) approach to represent the wind farm forces in the domain, and is coupled to a linearized background Navier–Stokes model of the ABL that allows for a representation of boundary-layer development over the wind farm, stratification effects, and gravity waves. Comparison of the wind farm power output of the TLM and LES results show very good agreement, with total wind farm power output and the trends of the power reduction across the windfarm rows matching well between the two codes. The comparison is made utilizing Conventionally Neutral Boundary Layers flowing across the TotalControl reference wind power plant rotated by different amounts to mimic different wind directions. Good comparison is observed in all the simulated cases.

REFERENCES

- Allaert D. & Meyers J. (2015). Large eddy simulation of a large wind-turbine array in a conventionally neutral atmospheric boundary layer. *Physics of Fluids* **27**, 065108.
- Allaerts D. & Meyers J. (2017). Boundary-layer development and gravity waves in conventionally neutral wind farms. *Journal of Fluid Mechanics* **814**, 95 – 130.
- Allaerts, D. and Meyers, J. (2019), Sensitivity and feedback of wind-farm induced gravity waves, *J. Fluid Mech.*, **862**, 990–1028.
- Andersen, S. J., Madariaga, A., Merz, K., Meyers, J., Munters, W., & Rodriguez, C. (2018). Reference Wind Power Plant D1.03. DTU Technical Report.
Online available at: http://orbit.dtu.dk/files/164663085/TotalControl_D1_03_Reference_Wind_Farm.pdf
- Bak C. et al. (2013). The DTU 10-MW Reference Wind turbine. DTU Technical Report.
Online available at: <http://dtu-10mw-rwt.vindenergi.dtu.dk/>
- Calaf M., Meneveau C. & Meyers J. (2010). Large eddy simulation study of fully developed wind-turbine array boundary layers. *Physics of Fluids* **22**, 015110.
- Munters W. & Meyers J. (2018). Optimal dynamic induction and yaw control of wind farms: effects of turbine spacing and layout. *Journal of Physics: Conference Series*, 0320125.
- Munters W., Meneveau C. & Meyers J. (2016). Turbulent inflow precursor method with time-varying direction for large-eddy simulations and applications to wind farms. *Boundary-layer Meteorology*, 305 – 328.
- Niayifar, A. and Porté-Agel, F. (2016), Analytical modeling of wind farms: A new approach for power prediction, *Energies*, **9**, 741.
- Vitsas A. & Meyers J. (2016) Multiscale aeroelastic simulations of large wind farms in the atmospheric boundary layer. *Journal of Physics Conference Series*, 753:082020, 2016.